

A Numerical Study on The Three Point Bending Behavior of Aluminum Foam Filled Stainless Steel Tube

Md Anwarul Hasan^{**}, Amkee Kim[†], Seong-Sik Cheon^{*}, Chang-Hun Lee^{**},
Hyo-Jin Lee^{***} and Seong-Seock Cho^{****}

알루미늄 폼으로 충전된 스테인레스 관의 3점 굽힘 특성에 관한 수치적 연구

하 산, 김엄기, 전성식, 이창훈, 이효진, 조성석

Key Words : Aluminum foam(알루미늄 폼), Foam filled structure(폼 충전 구조물),
Crashworthiness(충격 흡수능), Bending behavior(굽힘 거동), Finite element analysis
(유한요소해석)

Abstract

A comprehensive numerical study on the three point bending behavior of Aluminum foam-filled stainless steel tube has been performed. Aluminium alloy foams with various densities were produced and their mechanical properties were evaluated. Finite element(FE) analysis of three point bending test was performed to evaluate bending behavior of foam filled cylindrical structures. Results showed that foam filling offered remarkable increase of bending resistance and enhanced the crashworthiness of the structure. It turned out to prevent the inward fold formation at the compression flange, resulted into the multiple propagating folds and increased the load carrying capacity.

1. Introduction

Recent development of cost-effective processes for the production of low density metal foam such as powder metallurgical method has greatly increased the interest for its use in energy absorbing devices to reinforce the light weight structural members⁽¹⁾ in such diverse fields as automotive, transport, ships and military applications where weight reduction and high energy absorption are simultaneously required.

During the last two decades, extensive experimental theoretical and numerical work has been carried out in order to establish reliable design formulas⁽²⁻⁴⁾ and

software⁽⁵⁾ for prediction of energy absorption during crushing of thin walled column of various cross sections.

Santosa and Weirzbicki analyzed the crushing behavior of foam filled columns in the bending collapse mode using finite element code PAM-CRASH. Seizberger et al. performed numerical studies using explicit code ABAQUS^(6,7) while Hanssen, Hopperstad and Langseth performed a series of detailed studies on crashworthiness of foam filled members using LSDYNA^(8,9).

In this paper we have analyzed the three point bending behavior of Al-alloy filled circular stainless steel tube using the finite element code LSDYNA. Al-5wt%Si-4%Cu-4%Mg-1%TiH₂ alloy 544 foam was produced by powder metallurgical method. To obtain the mechanical properties of foam for using as input in the finite element code, the compression test was performed on several foam samples and the result was used to solve the scaling laws of foams. Numerical simulation was performed for different density foams. Result obtained from simulation showed that foam

[†] 공주대학교 기계공학부

E-mail : amkee@kongju.ac.kr

TEL : (041)850-8616 FAX : (041)854-1449

* 공주대학교 기계공학부

** 공주대학교 기계공학과 대학원

*** 한밭대학교 건축공학부

**** 충남대학교 신소재공학부

filling altered the bending behavior of stainless steel tube. It prevented the inward fold formation at the compression flange, resulted in multiple propagating folds and thus increased the load bearing capacity. Remarkable increase in bending moment resistance was obtained by Al-alloy foam filling.

2. Experiment

2.1 Material

The materials used in the study was alloy 544 (Al-5%Si-4%Cu-4%Mg) foams. The foams were produced using powder metallurgical method. Foam samples were obtained by foaming the alloy precursors in a mould keeping them for 15 min inside the furnace preheated at a temperature of 700^o C. Density of foam was controlled by varying amount of precursor material in the mould.

2.2 Compression test

Skin was removed from these foams and specimens were cut to the appropriate dimension (35 x 35 x 40 mm) using a band saw with a guide to ensure that the cuts were made accurately and straight. For obtaining the mechanical properties of foams the uni-axial compression test was performed on the specimens using an MTS 830 machine. Load was applied at a constant displacement speed of 0.02 mm/s and the compression was stopped when 85 % strain was reached.

2.3 Three point bending model

Fig. 2 shows the configuration of three point bending model used in the study. The model consisted of a foam filled stainless steel tube with two supports and a punch. The diameter of punch was 18 mm. The center to center distance between the two supports was 180 mm and the steel punch was located to impose force at the center of specimen. the maximum displacement of punch was set to be 48 mm. Length of each tube was 240 mm, the outer diameter being 38.4 mm and wall thickness 1.2 mm. Three different types of specimens were considered by using 1 PC (piece wise), 3 PC and 4 PC foam filler and for each of these types, foams of three different densities were used.

Fig. 3(a) shows the front isometric view of the numerical model while Fig 3(b) shows the rear isometric view of the model with 1 PC filler. In case of 1 PC filler specimen only the central part of tube was filled with foam, length of the foam filler being 120 mm. Fig 3(c) and (d) show the models with 3 and 4 PC filler respectively.



Fig. 1 Compression test specimen of alloy 322 foam, $\rho/\rho_s = 0.23$

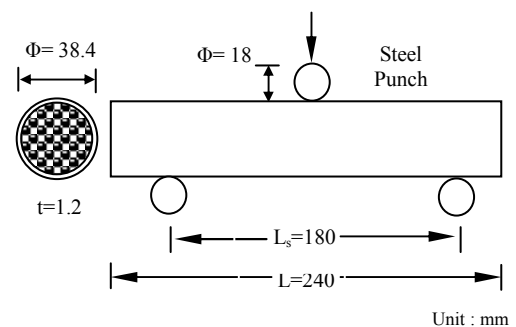


Fig. 2 Configuration of three point bending test (Experimental Setup)

2.4 Finite element modeling

Numerical analysis was carried out in the present paper using the non-linear explicit finite element code LS-DYNA. Considering the YOZ plane of symmetry, a half model, $L=240$ mm and half cross sectional area $\Phi = 38.4$ mm, as shown in Fig. 3(a)-(d), was used in the analysis to save the computation time.

The tube was represented using the default shell element of LS-DYNA but the foam elements were generated manually. The foam consisted of a total 1152 shell elements while the tube consisted of 384 shell elements.

The Hughes-Liu 4 node thin shell elements were used for the tube. To take the effect of transverse shear into consideration a shear correction factor of 0.8333 was assumed as recommended for isotropic material. A three-point through thickness integration scheme was applied for the shell elements. The foam cores were modeled with 8-node solid elements. Punch and supports were represented by rigid shell elements. Symmetric boundary conditions were applied to the XOZ and YOZ planes. For all elements stiffness based hourglass control was used in order to avoid unrealistic

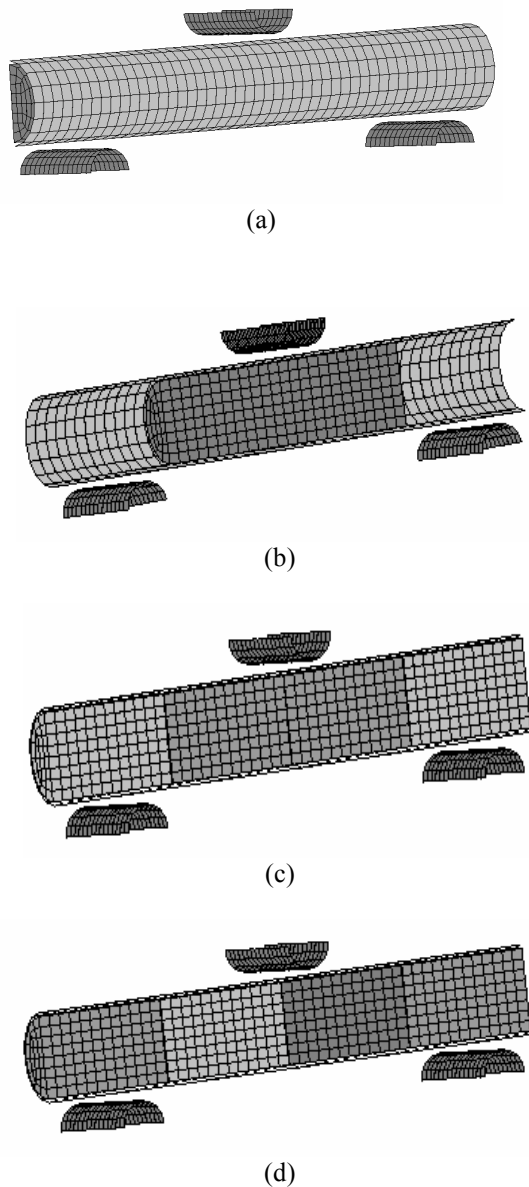


Fig. 3 Three point bending model for simulation (a) Front isometric view; (b), (c) and (d) rear isometric views

zero energy mode.

The interaction between the foam filler and tube wall was simulated with automatic surface to surface contact algorithm. The master-slave contact and self contact algorithm was applied to prevent the model from interpenetrating. The friction coefficient of 0.3 was used in this study. Foam skin has a substantial effect on bending behavior and strength. In the simulation, the skin was represented by shell elements around the foam core sharing common nodes with the foam surface.

2.5 Material modeling

The constitutive behavior of the thin shell element of

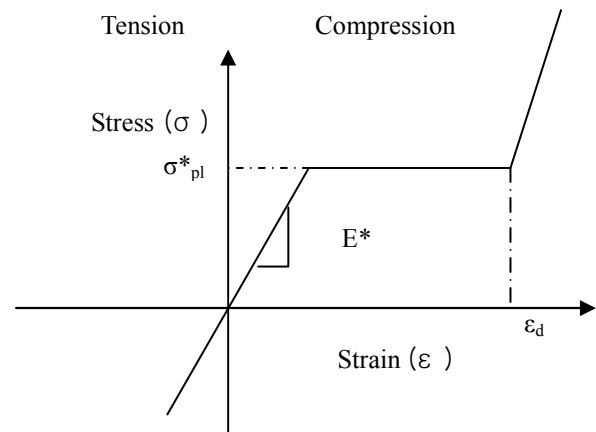


Fig. 4 Ideal stress-strain curve of aluminum alloy foam

the pipe was based on an elasto-plastic material with the mechanical properties Young's modulus, $E = 193 \text{ Gpa}$, yield stress, $\sigma_y = 210 \text{ MPa}$, Poisons ratio, $\nu = 0.29$ and mass density, $\rho = 7.8 \text{ gr/cm}^3$.

The material properties of skin were assumed to be same as those of the alloy before foaming and were obtained from tensile test on the precursor material.

Al foam core was modeled with the honeycomb material. The density of the foam fillers used in the simulation (without removing the skin) was in the range of 0.8 to 1.15 gm/cm^3 . From these densities, the density of foam without skin was calculated taking the skin thickness into consideration.

The corrected foam density was in the range of 0.26 to 0.94 gm/cm^3 . To obtain the mechanical properties of foam in this density range, uni-axial compression test was performed on several foam samples and then scaling laws^[10] as given by Eqns. 1 and 2 were solved for values of C_1 and C_2 . For the value $\phi = 0.6$ the values of C_1 and C_2 were 0.035 and 0.28 respectively. The engineering stress-strain curves for foams of various densities were then constructed using the values of E^* , σ_{pl}^* and ϵ_d obtained from Eqns. 1 to 4. An ideal engineering stress-strain curve of aluminium foam is shown in Fig. 4.

$$\frac{E^*}{E_s} = C_1 \phi^2 \left(\frac{\rho^*}{\rho_s} \right)^2 + C_1 (1 - \phi) \left(\frac{\rho^*}{\rho_s} \right) \tag{1}$$

$$\frac{\sigma_{pl}^*}{\sigma_y} = C_2 \left(\phi \frac{\rho^*}{\rho_s} \right)^{3/2} + C_2 (1 - \phi) \left(\frac{\rho^*}{\rho_s} \right) \tag{2}$$

$$\epsilon_d = 1 - \frac{1}{4} \left(\frac{\rho^*}{\rho_s} \right) + 0.4 \left(\frac{\rho^*}{\rho_s} \right)^3 \tag{3}$$

$$G^* = \frac{3}{8} E^* \tag{4}$$

In above set of Eqns. E_s , σ_y and ρ_s are elastic modulus, yield stress and mass density of solid cell wall of the foam material, ϕ is the volume fraction of solid contained in the cell edges while E^* , σ_{pl}^* and ρ^* are elastic modulus, yield stress and mass density of foam.

In the simulation, the behavior of foam was taken to be isotropic i.e. all the three directions were assumed to have the same mechanical properties. The shear elastic modulus was taken to be 3/8 of the compressive elastic modulus and the plastic shear strength was taken to be a half of the plastic collapse (plateau) stress.

3. Results and Discussion

3.1 Bending moment versus deformation angle

Fig. 5, 6 and 7 shows the bending moment vs deformation angle curve of 1 PC, 3 PC and 4 PC specimens respectively along with the curve for hollow tube. The curves in the figures show an initial linear elastic region where bending resistance increases rapidly with the deformation angle, followed by a plastic deformation region where the rate of change of resistance decreases slowly until a maximum bending resistance is reached. In the linear elastic region deformation of both foam and tube are elastic, and the bending moment of specimen is increasing elastically with deformation. After a certain deformation angle the non-linear deformation starts in the specimen and its bending behavior is governed by the configuration of specimen because of the different interaction between the foam core and the tube. After all, the bending moment continues to decrease till the end of the experiment.

Results showed that the bending moment resistance of foam filled specimens are much higher than that of hollow tube. For same type of foam filled specimens high density foam filler resulted in higher bending moment resistance. The maximum bending moment resistance among all the specimens was approximately 1200 Nm which is about 5 times that of hollow stainless steel tube (250 Nm). The partially filled 1 PC specimen (Fig. 5) showed much lower bending resistance compared to 3 PC and 4 PC foam filled specimens.

The simulation on 1 PC, 3 PC and 4 PC specimens with same density foams ($\rho_f / \rho_s = 0.23$) revealed that 3 PC specimen offered higher bending resistance than 1 PC and 4 PC filler specimens.

This may be because, in case of 4 PC filler specimen the punch axis during deformation falls at the interface between two foam fillers, so the foam pieces are likely to move apart slightly from each other. Consequently, in 4 PC filler specimens bending will occur easily showing lower bending resistance than 3 PC filler

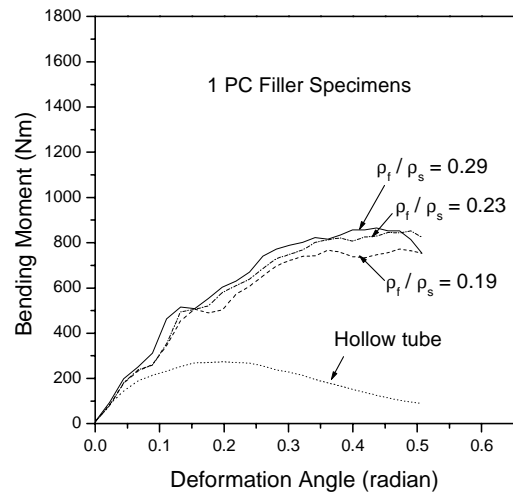


Fig. 5 Three point bending response of 1PC

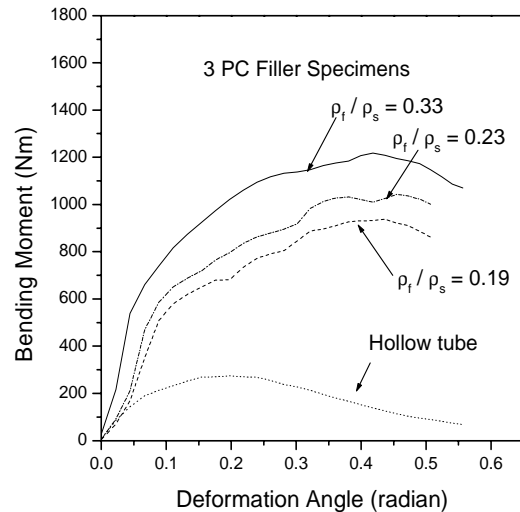


Fig. 6 Three point bending response of 3 PC

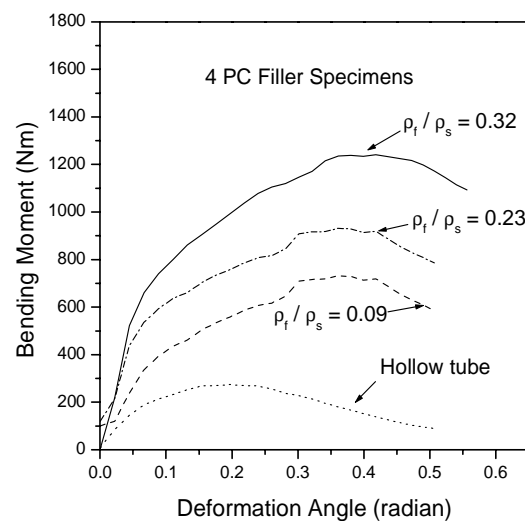


Fig. 7 Three point bending response of 4PC

specimens.

3.2 Behavior of bending deformation

The numerically obtained solid deformation pattern of hollow tube and foam filled (1 PC and 3 PC) tubes are shown in Figs 8 to 10 while Fig. 11 and 12 represent a mesh model of 4PC filler specimen before and after deformation. A solid model of deformation pattern of 4 PC filler specimen is shown in Fig. 13. Fig. 8 shows that the bending collapse of hollow cylindrical tube is a deep collapse which occurs at a section along a hinge line just below the punch axis, but the collapse in foam

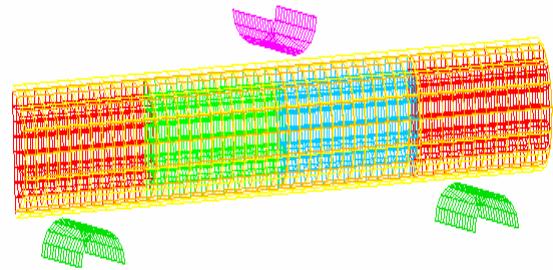


Fig. 11 Mesh model of 4 PC filler specimen before applying the load



Fig. 8 Deformation pattern of the hollow cylindrical Tube

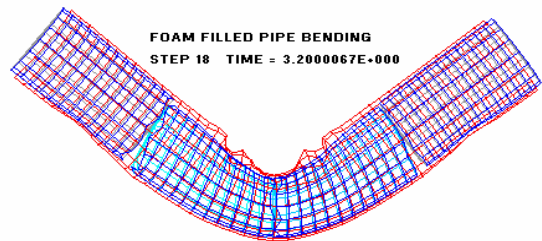


Fig. 12 Mesh model of final deformed shape of 4 PC filler specimen



Fig. 9 Deformation pattern of 1 PC foam filled cylindrical Tube

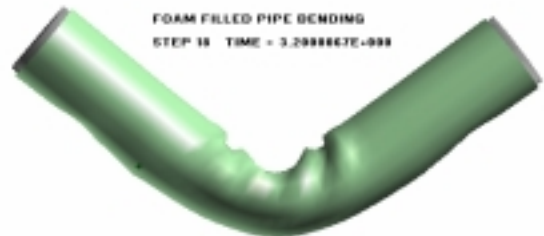


Fig. 13 Solid Deformation pattern of 4 PC foam filled cylindrical Tube

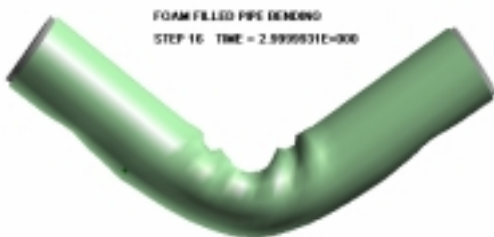


Fig. 10 Deformation pattern of 3 PC foam filled cylindrical Tube

filled tubes in Figs. 9, 10 and 12 are a combination of progressive folding and bending collapse of tubes.

The aluminium alloy foam filler retards the inward fold formation at the compression flange by providing lateral support to the tube wall. As a result the compressive flange forms additional outward folds in the next adjacent region along the length of the tube.

Thus the sectional collapse of tube along hinge line is retarded and progressive fold formation occurs giving rise to the bending resistance for same deformation angle and also increasing the energy absorption.

4. Conclusion

Finite element analysis was performed to simulate the bending behavior of foam-filled tubes using the explicit FEA code LSDYNA. The results are summarized as follows:

(1) Aluminum alloy foam filling increases the bending resistance of thin walled cylindrical tubes by retarding sectional collapse and giving rise to progressive fold formation.

(2) For same type of specimens (i.e. for any of the 1 PC, 3 PC, or 4 PC filler specimen) the maximum bending moment resistance is proportional to the relative density of foam filler.

(3) Bending resistance of the 3 PC filler specimens is higher than 1 PC and 4 PC filler specimens.

Acknowledgement

The authors wish to acknowledge the financial support of the Korea Science and Engineering Foundation by grant No. R01-2002-000-00093-0(2002) from its basic research program.

References

- (1) Kunze H.D, Baumeister J. Banhart J.Weber M, 1993, *Powder Met. Int.* Vol. 25, No. 4, pp. 182
- (2) T. Wierzbicki and W. Abramowicz, 1983, *J. of Appl Mech*, Vol. 50, pp. 727-739.
- (3) W. Abramowicz, and N. Jones, 1990 *Int J. Impact Engg*, Vol 9, No. 3, pp. 289-316
- (4) M. Langseth, and O.S. Hopperstad, 1999, *Int J. Impact Engg*, Vol. 18, No. 7-8, pp. 949
- (5) Crash-Cad, Licensed by Impact Design Inc., Winchester, MA
- (6) M. Seitzberger, F.G. Rammarstorfer, H.P. Desigscher and R. Gradinger, 1997, *Acta Mechanica*, Vol. 125, pp. 93-105
- (7) HKS, ABAQUS/Explicite User's Manual, 1996,Version 5.6,
- (8) A.G Hanssen, O.S. Hopperstad and M. Langseth, 1998, SUSI Conf. Greece.
- (9) J.O. Hallquist, 1998, Theoretical Manual, Livermore Soft. Tech. Corp.
- (10)M. F. Ashby, A. G. Evans, N. A. Fleck, L. J. Gibson, J.W. Hutchinson and H.N.G Wadley, 2000, *Metal Foams-A Design Guide*, Butterworth Heinemann, Boston, pp. 53.